Int j simul model 24 (2025) 2, 357-368
Original scientific paper

CONTROL OPTIMIZATION OF TURBOCHARGED DIRECT INJECTION MILLER CYCLE HYBRID ENGINE

Chen, L.-C.[*]; He, H.-W.[*,#]; Zhang, X.[**] & Hu, Z.-Q.[**]
[*] Beijing Institute of Technology, Beijing, China
[**] Beijing Jiaotong University, Beijing, China
E-Mail: lcchen2011@126.com, hwhebit@bit.edu.cn, zhangxin@bjtu.edu.cn, zhqhu@bjtu.edu.cn
([#] Corresponding author)

Abstract
Hybrid internal combustion engines need to optimize fuel consumption while increasing engine power, to achieve higher overall fuel economy and total range while ensuring charging performance. This paper takes a turbocharged direct injection Miller cycle hybrid engine as the research object, utilizing GT-Power to establish a one-dimensional simulation model. Through this model, the influence of the intake valve closing (IVC) advance angle on engine performance and combustion is studied. The results showed that in the high load region, the advance of IVC brought significant decrease in exhaust temperature, AI50 and ignition angle, which resulting in a significant increase in combustion speed, a decrease in ignition delay and combustion duration angle. In the end, with advanced IVC angle, the brake thermal efficiency increased 4.5 %. Meanwhile, the research outcome can be used to guide the calibration and shorten the development time.
(Received in February 2025, accepted in May 2025. This paper was with the authors 5 weeks for 2 revisions.)

Key Words: Miller Cycle, Combustion Simulation, Thermal Efficiency, Intake Efficiency

1. INTRODUCTION

Since the mid-20th century, the automotive industry has undergone unprecedented changes, among which advances in engine technology have been a key driving force for industry development [1]. The convergence and accelerated growth of electric vehicles and smart transportation are spurring technological transformations in both traditional engine-powered systems and engine-dependent hybrid technologies [2-4]. Since July 2021, China has implemented *GB19578-2021 "Limits for Fuel Consumption of Passenger Cars"*, which specifies the requirement to reduce the fuel consumption limit of passenger cars from 5 L / 100 km to 4 L / 100 km within 5 years [5]. Meanwhile, urbanization has contributed to an increase in the transport activities, and thus to a greater degradation of air quality in the European Union (EU) countries in recent years [6]. To achieve those goals, there are three technological routes available. The first one is Connectivity and Intelligence, some research focus on Connected and Automated Vehicles (CAVs) time headway and freeway speed limit impact to emission and fuel economy [7, 8]. The second one is developing electric vehicles and hydrogen energy technologies which reach zero CO_2 emission [9]. The last technical route is optimizing combustion technologies, such as fully variable valve control, variable compression ratio [10], Miller cycle [11, 12], etc., which improve the thermal efficiency of gasoline engines and reduce fuel consumption, have become research hotspots. Besides, since experimental research normally took long time and cost a lot, simulation research plays more and more important role on new combustion technology research aimed at fuel consumption, emission [13].

In reality, the three aforementioned technological pathways converge and synergistically enhance fuel efficiency and emission reduction. Particularly noteworthy is the integration of electric vehicle technology with internal combustion engine systems, which has given rise to hybrid electric vehicles (HEVs) and plug-in hybrid electric vehicles (PHEVs). HEVs and

PHEVs play a crucial role in achieving fuel consumption and emission targets, with control strategies forming the technical core and primary research focus for these vehicles [14, 15]. However, regardless of the sophistication of control technologies employed, the overall performance of HEVs and PHEVs remains fundamentally dependent on the intrinsic capabilities of their dedicated hybrid engines [16]. Most current HEV and PHEV specialized engines adopt either the Miller cycle or Atkinson cycle to optimize energy conservation and emission reduction [17]. The demonstrated advantages of the Miller cycle in turbocharged engines have attracted substantial research attention towards enhancing its operational efficiency and control effectiveness [18].

The Miller cycle engine achieves decoupling of compression ratio and expansion ratio by adjusting the timing of intake valve closure [19], thereby increasing the expansion ratio while maintaining the original compression ratio, effectively improving the thermal efficiency of the engine [20]. Many scholars have conducted research on the impact of Miller cycle on internal combustion engine performance through experimental [21] and simulation [22] methods. Xu et al. [23] analysed the mechanism by which the Miller cycle improves the thermal efficiency of a turbocharged direct injection gasoline engine. Under the advanced intake valve closing strategy, the Miller cycle reduces pump mean effective pressure under partial load conditions, improves mechanical efficiency, reduces heat transfer loss in the cylinder, and promotes fuel consumption improvement. Perceau et al. [24] found through zero-dimensional model simulation that the fuel saving rate of Miller cycle can reach 4 %; Li et al. [25] experimentally compared the performance under low and high load conditions. The results demonstrated that the Miller cycle reduced the fuel consumption rate by 4.7 % compared to the original engine configuration at high loads. At low loads, synergistically increasing the compression ratio with the Miller cycle achieved a fuel economy improvement of up to 7.4 %, which show that Miller cycle is beneficial for improving engine economy.

On the other hand, the Miller cycle can effectively reduce knocking under high load conditions and improve the fuel economy of the engine [26]. However, the Miller cycle has typically been paired with a larger physical compression ratio (13 or higher) to achieve an expansion ratio greater than the compression ratio [27], and due to the early closing of the intake stroke, the intake volume is lower at the same intake manifold pressure, resulting in a maximum torque and maximum power that is about 20 % to 30 % lower compared to Otto cycle engines of the same displacement [28].

At present, there is relatively little research on the effects of medium speed (3000 rpm), medium high load conditions of Miller cycle hybrid engines [29]. Meanwhile, more and more China carmakers start developing Range Extend Electric Vehicle (REEV) [30], which requires the engine running more often under medium speed area to charge the battery and drive the e-motor in parallel [31]. Increasing the maximum boost pressure of the intake system and appropriately reducing the physical compression ratio to increase the maximum power become the next research direction [32]. This paper is based on a 1.5-liter low compression ratio, high maximum torque (300 Nm) Miller cycle hybrid engine and conducts simulation studies on intake efficiency, air pump loss, effective compression ratio, exhaust temperature, ignition angle, ignition delay, combustion duration, AI50, maximum combustion pressure, thermal efficiency and boost response under low/medium/high load conditions at engine speed 3000 rpm.

2. METHOD

This paper uses GT-Power software to simulate and model the various subsystems and combustion processes of the Miller cycle hybrid engine in detail. The model is verified with actual test results. Finally, this model is used for variable parameter research.

2.1 Main technical parameters

The Miller cycle engine adopts valve early closing technology to achieve an effective compression ratio smaller than the effective expansion ratio, thereby improving the thermal efficiency of the engine. The exhaust lift angle is 276°CA (crank angle) and an intake lift angle of 233°CA. Meanwhile, the valve lift for both intake and exhaust are 9 mm, and the adjustment range for intake valve closing timing is 15°CA. Other key parameters are shown in Table I.

Table I: Key parameters of turbocharged direct injection Miller cycle hybrid engine.

Number of cylinders	4
Cylinder arrangement type	In line
Ignition sequence	1-3-4-2
Cylinder diameter (*d*)	75 mm
Stroke (*s*)	84 mm
Connecting rod length (*L*)	139.2 mm
Compression ratio (*ε*)	12

The calculation formula for the effective compression ratio r_c of Miller cycle is shown in Eq. (1):

$$r_c = \frac{V_{IVC}}{V_{TDC}} \tag{1}$$

In the formula, V_{IVC} is the cylinder volume when the intake valve is closed; V_{TDC} is the combustion chamber volume. Based on the relevant knowledge of internal combustion engines, it can be inferred as Eqs. (2) to (3):

$$V_{TDC} = \pi \cdot \frac{d^2}{4} \cdot \frac{s}{(\varepsilon - 1)} \tag{2}$$

$$V_{IVC} = \pi \cdot \frac{d^2}{4} \cdot \frac{s}{(\varepsilon - 1)} + \pi \cdot \frac{d^2}{4} \cdot \frac{s}{2} \cdot [1 + \cos(IVC)] \tag{3}$$

IVC is the intake valve closing advance angle, which is 0 when the valve closes at the intake bottom dead center. Substituting Eqs. (2) to (3) into Eq. (1) yields Eq. (4):

$$r_c = 1 + \frac{\varepsilon - 1}{2} \cdot [1 + \cos(IVC)] \tag{4}$$

From Eq. (4), the earlier the intake valve closes, the smaller its effective compression ratio. According to the principle of Miller cycle, it is known that it achieves the goal of reducing compression ratio and pumping loss by closing the valves early. Correspondingly, its disadvantage is the decrease in intake efficiency. This paper uses unit relative charge rl_u to characterize the intake efficiency of Miller cycle engines, which is defined as follows in Eq. (5):

$$rl_u = \frac{rl}{p - p_e} \tag{5}$$

In Eq. (5), *rl* represents the relative charge, *p* is the intake manifold pressure, p_e is the partial pressure of remain exhaust gas.

2.2 Establishment of simulation model

This paper uses GT-Power software to simulate and model the various subsystems and combustion processes of the Miller cycle hybrid engine in detail. A one-dimensional simulation model is built, and the overall model is shown in Fig. 1, mainly including the intake system, intercooler system, intake pipe, intake pipe, exhaust pipe, turbocharger, and exhaust system. The Chen-Flynn model

was used to calculate the engine friction work, the Weber combustion model based on AI50 was used to calculate the engine combustion process, and the SITurb model was used to calculate the influence of camshaft lift and opening/closing timing on the engine intake performance.

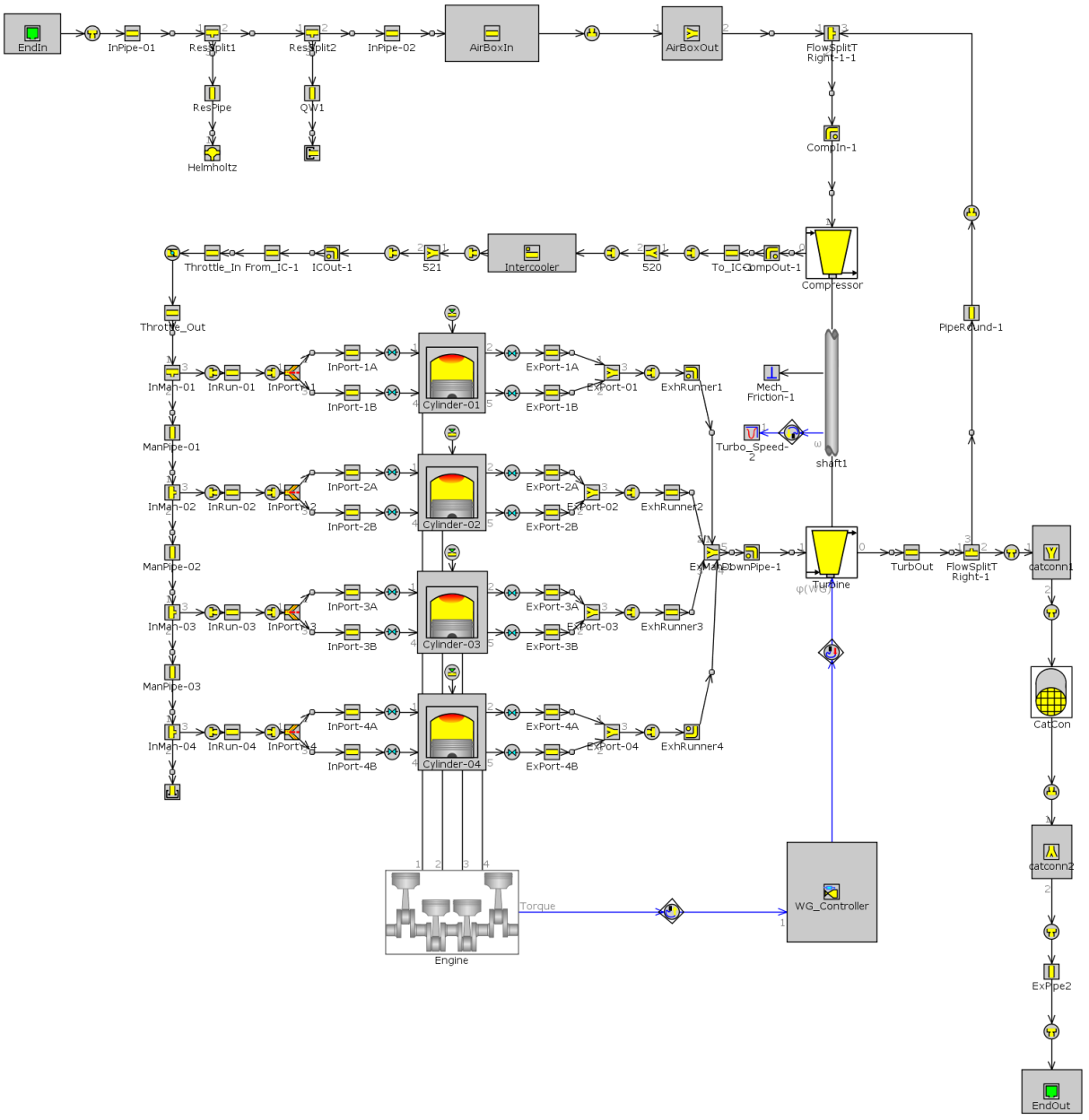

Figure 1: One dimensional simulation model of turbocharged direct injection Miller cycle hybrid engine.

2.3 Validation of simulation model

Selecting an engine speed of 3000 rpm and average effective pressures of 7 bar, 14 bar, and 300 Nm as simulation operating points, the cylinder pressure curve of the simulation model is recorded and compared with the actual measured engine cylinder pressure curve. The comparison results are shown in Fig. 2. The error between simulated cylinder pressure curve and the actual cylinder pressure curve does not exceed 5 %, which meets the requirements of subsequent simulation analysis.

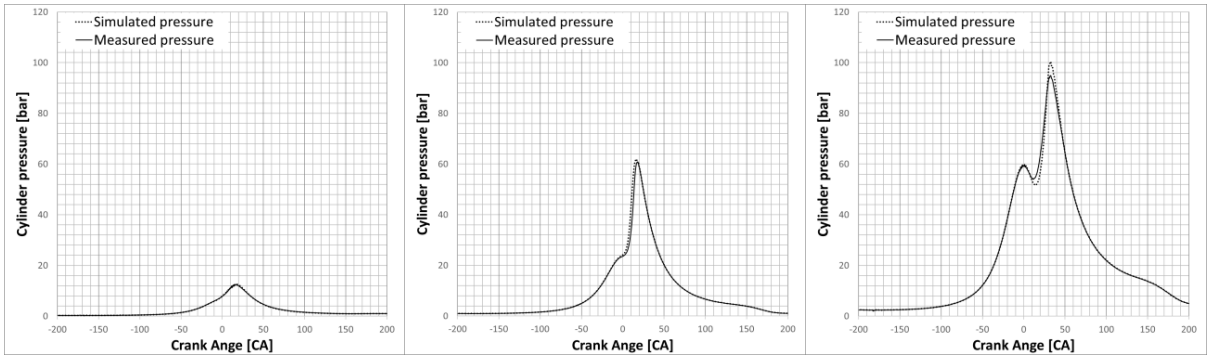

a) 3000 rpm, 7 bar b) 3000 rpm, 14 bar c) 3000 rpm, 300 Nm

Figure 2: Comparison between simulated cylinder pressure curve and the measured cylinder pressure curve at 3000 rpm, 7 bar, 14 bar, and 300 Nm.

3. RESULTS

The simulation analysis in this paper ensures consistent output average effective pressure or torque by adjusting the intake air volume and the ignition angle. When the *IVC* advance angle changes and causes a change in torque, the same torque can be achieved by adjusting the opening of the turbine exhaust valve. Meanwhile, the ignition angle shall be adjusted to achieve AI50 of 8°CA or the knocking index $k_{KITI} > 1$. The impact of *IVC* advance angle on intake efficiency, air pump loss, effective compression ratio, exhaust temperature, ignition angle, ignition delay, combustion duration, AI50, maximum combustion pressure, thermal efficiency and boost response has been analysed.

3.1 Analysis of intake efficiency

As shown in Fig. 3, with the advancement of *IVC*, there is a significant decrease in intake efficiency at various loads, and the intake efficiency at low loads is significantly lower than that at medium and high loads. Currently, due to the large proportion of exhaust gas partial pressure at low loads and the significant increase in intake pressure at medium and high loads, the proportion of exhaust gas partial pressure decreases, resulting in a relatively stable intake efficiency at medium and high loads.

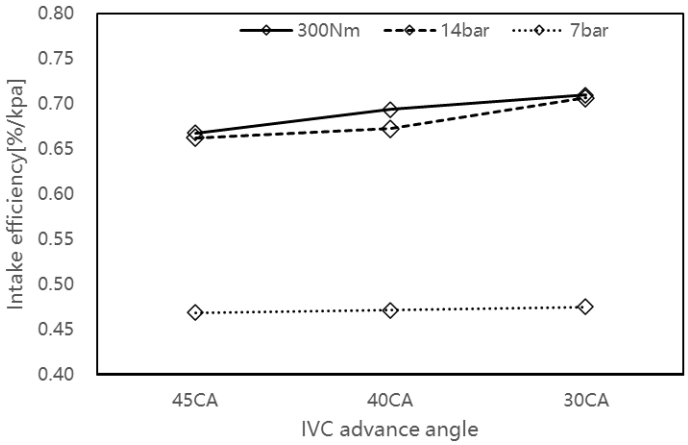

Figure 3: The influence of *IVC* advance angle on intake efficiency.

3.2 Analysis of air pump loss and effective compression ratio

Fig. 4 shows the variation of air pump loss and effective compression ratio with *IVC* timing. It can be seen from Fig. 4 that the earlier the *IVC* time, the lower the effective compression ratio. When

the engine is under low load (such as at an average effective pressure of 7 bar), the pumping loss decreases with the advance of *IVC*. On the contrary, when the engine is under medium to high load, the pumping loss hardly changes with the advance of *IVC*. This is because under low load, the intake manifold is in a negative pressure state, and after *IVC* is advanced, the required absolute pressure of the manifold at the same average effective pressure is higher, so the pumping loss is correspondingly reduced. Under medium to high loads, the intake manifold of a turbocharged engine is already in a positive pressure state, so the valve closing early and closing late almost does not affect the pumping loss.

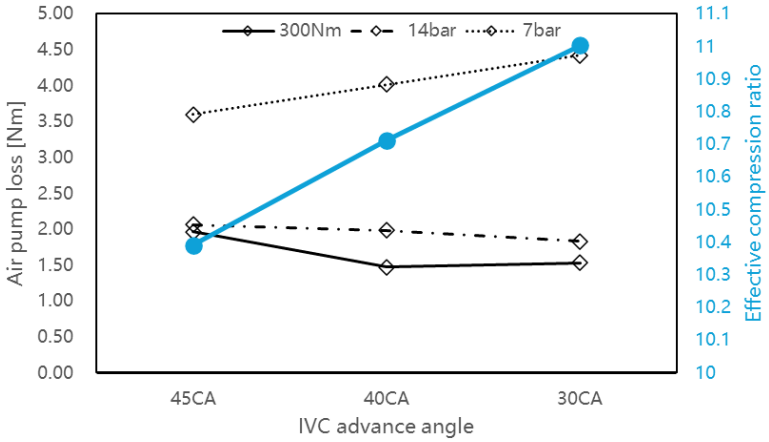

Figure 4: The influence of *IVC* advance angle on air pump loss and effective compression ratio.

3.3 Analysis of exhaust temperature and ignition angle

From Fig. 5, when the *IVC* timing is advanced, reducing the effective compression ratio is beneficial for lowering the combustion end temperature and exhaust temperature. Due to the higher exhaust temperature under medium to high loads, the decrease in exhaust temperature is more significant (at 300 Nm, the temperature drops 53 °C when the effective compression ratio reduces from 11 to 10.4). According to [25], exhaust temperature is one of the main factors causing knocking. Therefore, the ignition angle increases after the *IVC* timing is advanced, and it is more significant in the medium to high load region. The ignition angle under *IVC* advance of 45°CA is about 2.7°CA larger than that under 30°CA.

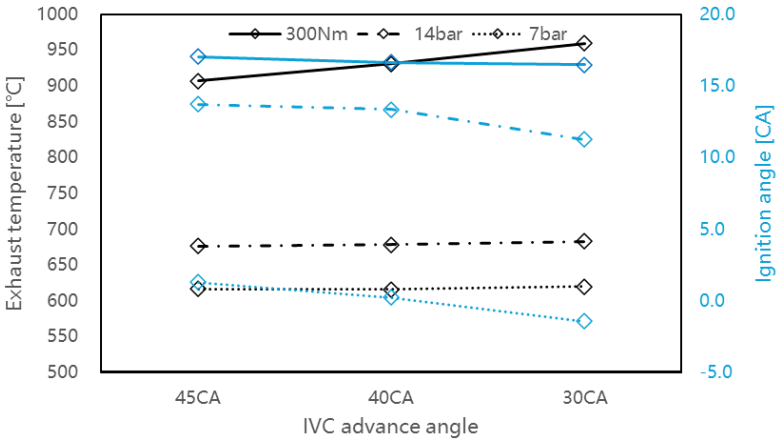

Figure 5: The influence of *IVC* advance angle on exhaust temperature and ignition angle.

3.4 Analysis of ignition delay and combustion duration

This paper characterizes the ignition delay period using the interval between ignition angle and AI05 and characterizes the combustion duration using the interval between AI05 and AI90. From

Fig. 6, with the advancement of *IVC*, the ignition delay period significantly increases under low load, but the combustion duration is almost the same. Under high load, as *IVC* advances, the ignition delay and combustion duration shorten. The trend of ignition delay and combustion duration with *IVC* under moderate load is not significant.

This indicates that the earlier the *IVC* under low load, the more adverse it will have on the small-scale turbulent kinetic energy in the cylinder. This effect leads to a slower formation of the initial combustion nucleus, but when the nucleus is fully formed, the pressure wave generated by the combustion itself is sufficient to promote the rapid propagation of the flame, so the combustion duration is not significantly affected. Under high load, due to the high intake manifold pressure, the small-scale turbulent energy in the cylinder is not greatly affected. On the contrary, due to the early *IVC* and Miller cycle, the ignition angle is significantly reduced, and the turbulent energy at the beginning of combustion is higher, which is conducive to the development of combustion.

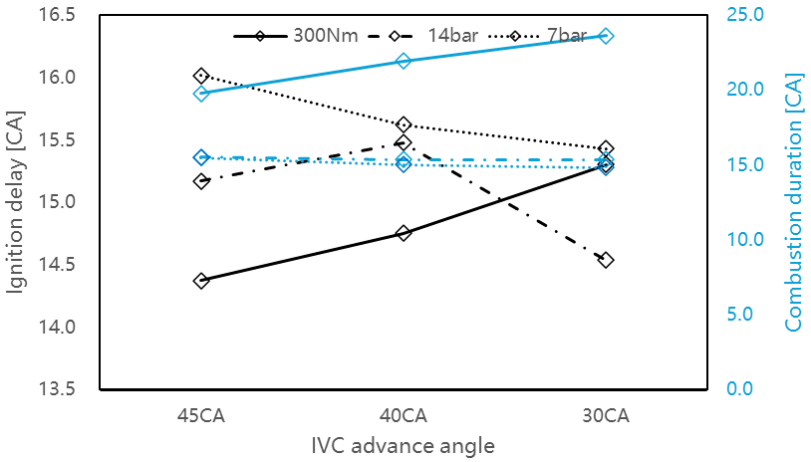

Figure 6: The influence of *IVC* advance angle on ignition delay and combustion duration.

3.5 Analysis of AI50 and maximum combustion pressure

From Fig. 7, there is a good negative correlation between maximum combustion pressure and AI50. Under high load, as *IVC* advances, the exhaust temperature decreases and the ignition angle becomes larger, resulting in earlier combustion and correspondingly smaller AI50. At the same time, the maximum combustion pressure is also higher. Under medium and low loads, due to the small difference in ignition advance angle, AI50 and maximum combustion pressure vary almost uniformly with *IVC*.

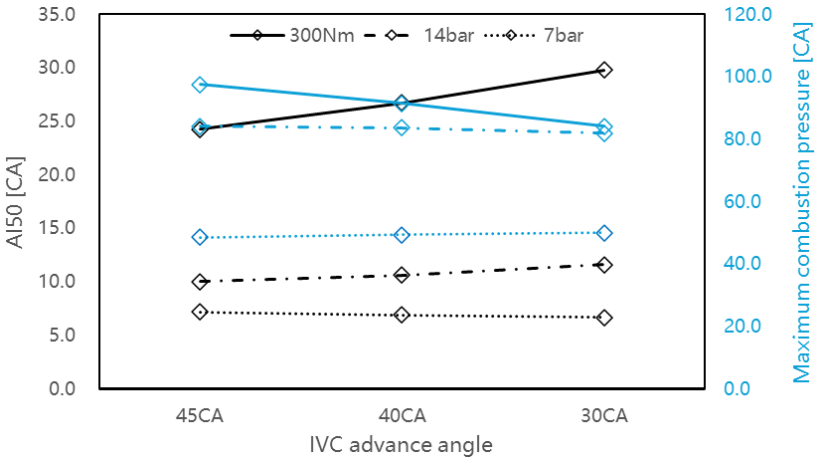

Figure 7: The influence of IVC advance angle on AI50 and maximum combustion pressure.

3.6 Analysis of thermal efficiency

There are two methods for evaluating thermal efficiency: one is brake thermal efficiency (*BTE*), which is calculated from engine net output power; the other is indicate thermal efficiency (*ITE*), which is calculated from engine indicated torque. The former is used to characterize the actual thermal efficiency of the engine (considering pump losses, friction losses, and accessory losses), while the latter is only used to characterize the combustion thermal efficiency of the engine. Since the *BTE* is more widely used for combustion efficiency evaluation, we take *BTE* as the analysis object.

According to Fig. 8, the highest thermal efficiency of the Miller cycle engine occurs in the medium load region, and its thermal efficiency increases with the advancement of *IVC*. Finally, compared to the later *IVC* angle, the brake thermal efficiency increases by 4.5 %, 0.9 %, and 1.5 % in the distribution of large, medium, and small loads.

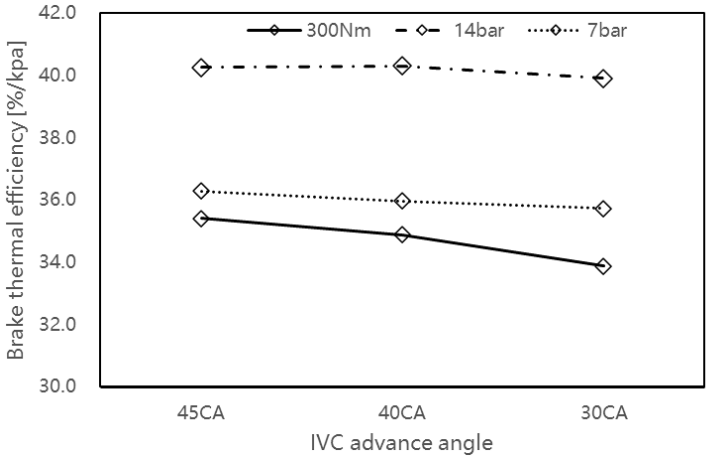

Figure 8: The influence of *IVC* advance angle on thermal efficiency.

3.7 Analysis of boost response

As mentioned earlier, the earlier the *IVC*, the more unfavourable it is for intake efficiency. For turbocharged engines, increasing the turbo speed and boost pressure at medium to high speeds can compensate for the lack of intake efficiency [33, 34]. However, at low engine speeds, the transient response degradation caused by the Miller cycle becomes more pronounced. Fig. 9 shows the earlier the *IVC* time, the slower boost response. Further analysis of the response in the first second reveals that the earlier the *IVC*, the faster the decrease in intake pressure in the first second and the earlier the inflection point, while the increase in boost pressure is faster compared to the later *IVC* angle. Mechanistic investigations indicate that advancing *IVC* timing elevates the effective compression ratio while reducing the initial in-cylinder charge mass. This dual effect intensifies pressure fluctuations in the intake manifold with pressure gradients exceeding baseline conditions, thereby shifting the pressure curve inflection point forward. Concurrently, the earlier compression process advances combustion phasing, enabling exhaust energy to act on the turbine sooner. This mechanism counteracts the turbocharger rotor's inertial lag by reducing the inertial time constant, which fundamentally explains the accelerated boost pressure buildup. This phenomenon underscores the coupled interaction between valve timing and thermodynamic processes in turbocharged systems: during transient conditions, optimized in-cylinder processes can overcome the response limitations imposed by turbocharger mechanical inertia through precise adjustment of exhaust energy release timing. Comparative analysis with correlational research confirms the consistency in observing *IVC* advancement's positive effect on boost response [35]. While their study highlights how high geometric compression ratios and exhaust gas recirculation amplify the Miller cycle's fuel economy benefits, the present work reveals that independent *IVC* timing

optimization. These findings jointly validate valve timing's pivotal role as a critical leverage mechanism in thermo-mechanical energy transfer chains.

Mapping the transient operating points onto the compressor efficiency map (Fig. 10) reveals that when *IVC* is advanced, the traversal operating points shift towards the lower left corner of the low efficiency area. The disadvantage of low initial intake efficiency is amplified in the instantaneous power response of turbocharged engines, resulting in lower turbo efficiency and slower torque establishment.

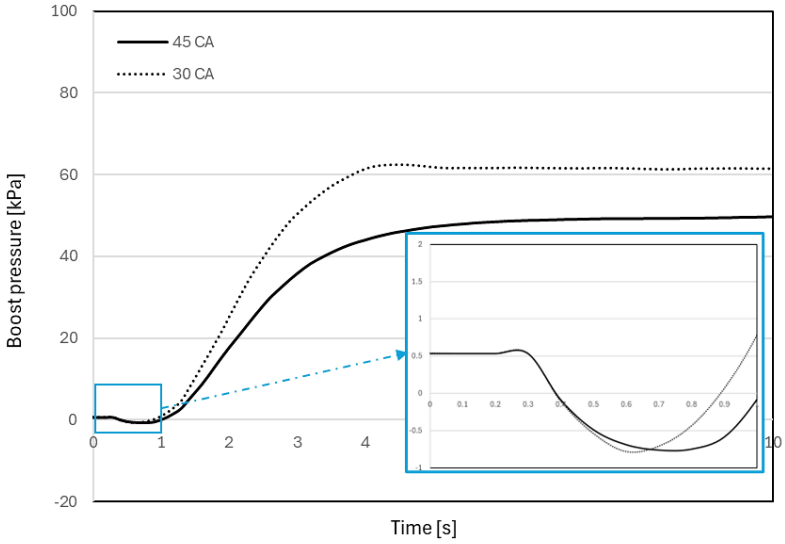

Figure 9: The influence of *IVC* advance angle on boost speed.

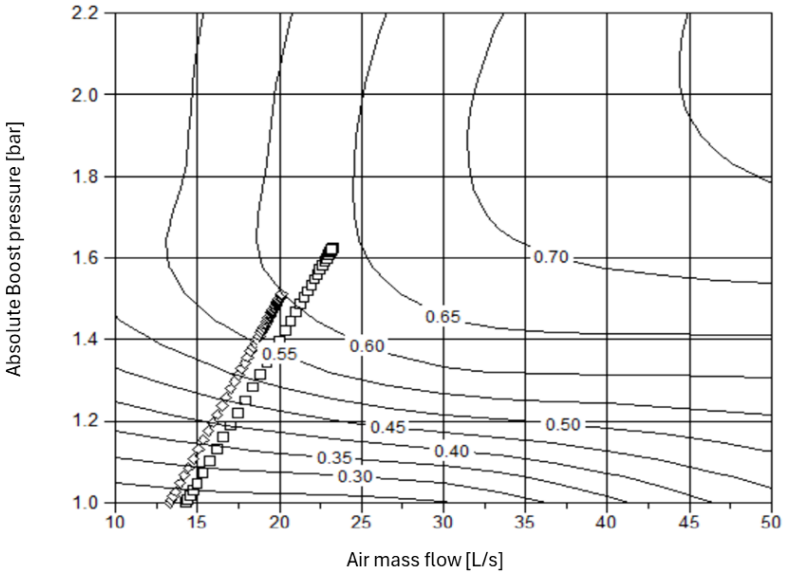

Figure 10: Distribution of transient operating conditions on compressor efficiency diagram.

4. CONCLUSION

The turbocharged direct injection miller cycle hybrid engine can effectively optimize combustion and thermal efficiency by adjusting the *IVC* angle, however, the reduction of intake efficiency has an obvious side effect to boost response.

In the low load region, the advance of *IVC* can effectively reduce pumping losses, prolong the ignition delay period, but the combustion duration does not change much, and AI50 and ignition angle do not show significant changes. Therefore, its indicate thermal efficiency does not change

significantly, but due to the reduction of pumping losses, the brake thermal efficiency increases by about 1.5 %.

In the medium load region, the advance of *IVC* has little effect on pump loss, ignition delay, and combustion duration angle. However, due to the decrease in exhaust temperature, AI50 and ignition angle are advanced, resulting in a slight increase in indicate thermal efficiency and a brake thermal efficiency by 0.9 %.

In high load areas, the advance of *IVC* has little impact on pump air loss. However, due to the significant decrease in exhaust temperature, both AI50 and ignition angle have been significantly advanced, resulting in obvious decrease in ignition delay and combustion duration, and a 4.5 % increase in indicated thermal efficiency and effective thermal efficiency.

The advance of *IVC* will reduce the intake efficiency, resulting in a decrease in the relative intake volume under the same intake pressure. Moreover, such a decrease will further lead to a decrease in the overall efficiency of the turbine during transient operating conditions, thereby amplifying its adverse effects. At low speeds, the impact of 15°CA on the turbine response exceeds 0.9 seconds, and the influence of *IVC* submission angle shows a nonlinear and rapid degradation trend.

REFERENCES

[1] Heywood, J. B. (2018). *Internal Combustion Engine Fundamentals*, 2nd ed., McGraw-Hill Education, New York

[2] Huang, A. Q.; Zhang, Y. Q.; He, Z. F.; Hua, G. W.; Shi, X. L. (2021). Recharging and transportation scheduling for electric vehicle battery under the swapping mode, *Advances in Production Engineering & Management*, Vol. 16, No. 3, 359-371, doi:10.14743/apem2021.3.406

[3] Li, J.; Li, J.; Fang, H; Jiang, J. (2024). Dynamic energy-efficient path planning for electric vehicles using an enhanced ant colony algorithm, *Technical Gazette*, Vol. 31, No. 2, 434-441, doi:10.17559/TV-20230510000618

[4] Wang, D. L.; Ding, A.; Chen, G. L.; Zhang, L. (2023). A combined genetic algorithm and A* search algorithm for the electric vehicle routing problem with time windows, *Advances in Production Engineering & Management*, Vol. 18, No. 4, 403-416, doi:10.14743/apem2023.4.481

[5] GB 19578-2021. (2021). *Fuel Consumption Limits for Passenger Cars*, China Standards Press, Beijing

[6] Petrović, N.; Bojović, N.; Marinković, D.; Jovanović, V.; Milanović, S. (2023). A two-phase model for the evaluation of urbanization impacts on carbon dioxide emissions from transport in the European Union, *Technical Gazette*, Vol. 30, No. 2, 514-520, doi:10.17559/TV-20221018103946

[7] Lu, Q.; Tettamanti, T. (2021). Impacts of connected and automated vehicles on freeway with increased speed limit, *International Journal of Simulation Modelling*, Vol. 20, No. 3, 453-464, doi:10.2507/IJSIMM20-3-556

[8] Petrescu, M.; Ștefan, M.-C.; Panagoreț, A. A.; Croitoru, I. O.; Chiriță, S.; Steriopol, B. C. (2024). Route planning and machine learning algorithms for sensor-equipped autonomous vehicles in agriculture, *Studies in Informatics and Control*, Vol. 33, No. 4, 105-112, doi:10.24846/v33i4y202410

[9] Niu, X.; Luo, X. (2024). Exploration of the diversified path of energy economic transformation based on the perspective of hydrogen energy industry innovation, *Technical Gazette*, Vol. 31, No. 4, 1179-1191, doi:10.17559/TV-20240201001307

[10] Wittek, K.; Geiger, F.; Andert, J.; Martins, M.; Cogo, V.; Lanzanova, T. (2019). Experimental investigation of a variable compression ratio system applied to a gasoline passenger car engine, *Energy Conversion and Management*, Vol. 183, 753-763, doi:10.1016/j.enconman.2019.01.037

[11] Jena, P.; Tirkey, J. V. (2024). Power and efficiency improvement of SI engine fueled with boosted producer gas-methane blends and LIVC-Miller cycle strategy: thermodynamic and optimization studies, *Energy*, Vol. 289, Paper 130068, 17 pages, doi:10.1016/j.energy.2023.130068

[12] Solomon, A.; Battiston, P.; Sczomak, D. (2021). Lean-stratified combustion system with Miller cycle for downsized boosted application – Part I, *SAE International Journal of Advances and Current Practices in Mobility*, Vol. 3, No. 4, 1666-1681, doi:10.4271/2021-01-0458
[13] Tarbajovsky, P.; Puskar, M.; Sabadka, D. (2023). Simulation model of vehicle emission reduction exhaust system, *International Journal of Simulation Modelling*, Vol. 22, No. 4, 679-689, doi:10.2507/IJSIMM22-4-675
[14] Wirasingha, S. G.; Emadi, A. (2010). Classification and review of control strategies for plug-in hybrid electric vehicles, *IEEE Transactions on Vehicular Technology*, Vol. 60, No. 1, 111-122, doi:10.1109/TVT.2010.2090178
[15] Yasin, M.; Abirami, M.; Kbvsr, S. (2024). Heuristic adaptive dynamic programming-based energy optimization strategies for hybrid electric vehicles, *Technical Gazette*, Vol. 31, No. 1, 145-150, doi:10.17559/TV-20230430000589
[16] Ban, L. (2024). Optimization of energy management algorithm for hybrid power systems based on deep reinforcement learning, *Studies in Informatics and Control*, Vol. 33, No. 2, 15-25, doi:10.24846/v33i2y202402
[17] Chen, B.; Zhang, L.; Han, J.; Zhang, Q. (2019). A combination of electric supercharger and Miller cycle in a gasoline engine to improve thermal efficiency without performance degradation, *Case Studies in Thermal Engineering*, Vol. 14, Paper 100429, 7 pages, doi:10.1016/j.csite.2019.100429
[18] Shen, K.; Xu, Z.; Chen, H.; Zhang, Z. (2021). Investigation on the EGR effect to further improve fuel economy and emissions effect of Miller cycle turbocharged engine, *Energy*, Vol. 215, Part B, Paper 119116, 11 pages, doi:10.1016/j.energy.2020.119116
[19] Kozlov, A. V.; Fedorov, V. A.; Milov, K. V. (2021). Improving the energy efficiency of a 6ChN13/15 gas engine with a Miller cycle by optimizing the valve timing, *Trudy NAMI*, Vol. 2021, No. 4, 41-52, doi:10.51187/0135-3152-2021-4-41-52
[20] Gumerov, I. F.; Fardeev, L. I.; Andriyanov, S. M.; Kozlov, A. V.; Matveev, A. A.; Milov, K. V. (2022). Thermodynamic analysis of an engine with compression ignition according to the controlled Miller cycle, *Trudy NAMI*, Vol. 2022, No. 3, 27-35, doi:10.51187/0135-3152-2022-3-27-35
[21] Zhu, D.; Wu, H.; Lee, T.; Sun, Q.; Shi, Z.; Li, X.; Lee, C.-F. (2024). Effects of the turbocharged Miller cycle strategy on the performance improvement and emission characteristics of diesel engines, *Environmental Pollution*, Vol. 346, Paper 123587, 12 pages, doi:10.1016/j.envpol.2024.123587
[22] Knelts, V. F.; Rumyancev, P. G. (2022). Reducing toxic emissions of diesel engines on the basis of the Miller cycle, *Russian Engineering Research*, Vol. 42, Suppl. 1, S49-S50, doi:10.3103/S1068798X23010112
[23] Xu, J.; Guo, T.; Feng, Y.; Sun, M. (2021). Numerical investigation of Miller cycle with EIVC and LIVC on a high compression ratio gasoline engine, *Science Progress*, Vol. 104, No. 2, Paper 00368504211023640, 17 pages, doi:10.1177/00368504211023640
[24] Perceau, M.; Guibert, P.; Guilain, S.; Segretain, F.; Redlinger, T. (2020). Why can Miller cycle improve the overall efficiency of gasoline engines?, *Proceedings of the THIESEL 2020 Conference on Thermo- and Fluid Dynamic Processes in Direct Injection Engines*, 18 pages
[25] Li, T.; Gao, Y.; Wang, J.; Chen, Z. (2014). The Miller cycle effects on improvement of fuel economy in a highly boosted, high compression ratio, direct-injection gasoline engine: EIVC vs. LIVC, *Energy Conversion and Management*, Vol. 79, 59-65, doi:10.1016/j.enconman.2013.12.022
[26] Wei, H.; Shao, A.; Hua, J.; Zhou, L.; Feng, D. (2018). Effects of applying a Miller cycle with split injection on engine performance and knock resistance in a downsized gasoline engine, *Fuel*, Vol. 214, 98-107, doi:10.1016/j.fuel.2017.11.006
[27] Xing, K.; Huang, H.; Guo, X.; Wang, Y.; Tu, Z.; Li, J. (2022). Thermodynamic analysis of improving fuel consumption of natural gas engine by combining Miller cycle with high geometric compression ratio, *Energy Conversion and Management*, Vol. 254, Paper 115219, 16 pages, doi:10.1016/j.enconman.2022.115219
[28] Wu, C.; Puzinauskas, P. V.; Tsai, J. S. (2003). Performance analysis and optimization of a supercharged Miller cycle Otto engine, *Applied Thermal Engineering*, Vol. 23, No. 5, 511-521, doi:10.1016/S1359-4311(02)00239-9

[29] Smirnov, S. V.; Makarov, A. R.; Zaev, I. A.; Khudaibergenova, G. T. (2021). Research of the efficiency of using the Miller cycle of an internal combustion engine, *RUDN Journal of Engineering Research*, Vol. 22, No. 2, 196-204, doi:10.22363/2312-8143-2021-22-2-196-204

[30] Liu, X.; Zhao, F.; Hao, H.; Liu, Z. (2023). Comparative analysis for different vehicle powertrains in terms of energy-saving potential and cost-effectiveness in China, *Energy*, Vol. 276, Paper 127564, 13 pages, doi:10.1016/j.energy.2023.127564

[31] Jing, J.; Liu, Y.; Huang, W.; Wu, J.; Zuo, B. (2020). Control of changed single motor torque output path transition in P2.5 hybrid system, *2020 3rd International Conference on Control and Robots (ICCR)*, 191-198, doi:10.1109/ICCR51572.2020.9344154

[32] Molina, S.; García, A.; Monsalve-Serrano, J.; Estepa, D. (2018). Miller cycle for improved efficiency, load range and emissions in a heavy-duty engine running under reactivity controlled compression ignition combustion, *Applied Thermal Engineering*, Vol. 136, 161-168, doi:10.1016/j.applthermaleng.2018.02.106

[33] Wang, R.; Qiao, J.; Jia, D.; Shen, D.; Duan, X.; Liu, J. (2024). Effects of asynchronous late intake valve closing combined with high geometric compression ratio and exhaust gas recirculation on combustion and fuel consumption in a turbocharged SI engine: an experimental study, *Energy*, Vol. 290, Paper 130058, 12 pages, doi:10.1016/j.energy.2023.130058

[34] Gonca, G.; Sahin, B.; Parlak, A.; Ust, Y.; Ayhan, V.; Cesur, I.; Boru, B. (2015). Theoretical and experimental investigation of the Miller cycle diesel engine in terms of performance and emission parameters, *Applied Energy*, Vol. 138, 11-20, doi:10.1016/j.apenergy.2014.10.043

[35] Jia, D.; Qiao, J.; Wang, S.; Liu, J.; Guan, J.; Wang, R.; Duan, X. (2025). The effect of variable enhanced Miller cycle combined with EGR strategy on the cycle-by-cycle variations and performance of high compression ratio engines based on asynchronous valve opening strategy, *Energy*, Vol. 320, Paper 135307, 16 pages, doi:10.1016/j.energy.2025.135307